International Journal for Housing Science and Its Applications
Publish August 3, 2025. Volume 46, Issue 3 Pages 768-779

https://doi.org/10.70517/ijhsa46357

Research on the development of high-definition photographic image compression and recovery technology innovation based on improved multi-objective optimization algorithm under all-media convergence

Yuliang Xiang[1,*]
[1] College of Commerce and Trade, Hunan Institute of Industrial Technology, Changsha, Hunan, 410208, China
Corresponding authors: (e-mail: x80274352@126.com).

Abstract The data volume of high-definition (HD) photographic images is proliferating, which puts forward higher requirements for efficient compression and high-quality recovery techniques, for which an innovative technique for all-media converged HD image compression and recovery based on improved multiple-external optimize algorithm is proposed. By improving the traditional genetic algorithm to acquire more advanced computational precision and faster convergence speed, the improved arithmetic is applied to optimizing the weightings and value range of the BP neuro mesh to enhance the generalization perform of the neuro mesh. And the combined pattern is applied to the HD camera image compression and recovery under the all-media convergence, which calculates and retains the image compression and recovery data, and reconstructs the HD image from the data blocks. The average GD and IGD of this paper's method are 0.0312 and 0.0703 for image compression and recovery strategy optimization, which are more advanced than the comparison ways. With the improvement of the degree of graphic compression, the image compression evaluation indexes of the method are improved to different degrees. For image 1, the PSNR of image compression of this method is 30.45db and MS-SSIM is 0.91, which is better than the pass comparison method. In five types of image recovery tasks, the PSNR of this paper's model is between 31.69 and 34.76db, and the SSIM is between 0.846 and 0.924, and the image recovery tasks can be accomplished excellently.

Index Terms Multi-objective optimization, Improved genetic algorithm, BP neural network, Image compression and recovery, Technological innovation

I. Introduction

Because of the optical basics of mankind sensory cognition of the earth, graphic is an crucial ways for mankind beings to acquire data, expression data and transmission data [1], [2]. In the context of all-media convergence, the dissemination and downloading of images will directly affect the overall quality of images, so the compression and recovery of high-definition (HD) photographic images are of great significance to ensure the quality of HD images [3], [4].

Image compression is the process of compressing an image file to make it smaller, while the quality of the image must not be distorted to an unacceptable degree, in order to save as many files as possible in a given storage space and to speed up the transmission of information over the network [5]-[7]. Graphic compress can be of all genres, wastage and non-loss compress respectively. Lossless compress is a compression method that enables complete and accurate reconstruction of an image without losing any information contained in the image [8], [9]. Lossy compression is a compression process that discards some of the less crucial data in the graphic, which is perfectly acceptable in many cases as long as these distortions are not noticeable to the human eye [10], [11]. This provides very favorable conditions for compression ratios, and the more losses the image quality allows, the greater the compression ratio that can be achieved [12]. Graphic compress is the basics of graphic store, dispose and transfer, it can decrease the stress of graphic store and transmission, so that the image on the mesh to realize speediness transfer and practical-time dispose [13]-[15]. And graphic recovery is to recover the compressed graphic to the pre-compress image to ensure that the quality of the image is not damaged [16], [17].

Literature [18] proposed new eyeless frail watermark way to detection tampering and recover tampered images better and utilized a new feature extraction scheme which revealed higher efficiency in detecting tampering and recovering the original image as compared to existing methods. Literature [19] describes a secure non-loss recover project for medicine graphic that incorporate all portion: shared dynasty and non-loss recover, aiming to protect the integrity of medical graphic information, verified to have better performance, even if the tampering rate is greater

than 50%, the primitive graphic can be regain non-loss. Literature [20] proposed a good-character recovery graphic encipherment arithmetic based on disperse cosine conversion (DCT) frequencies-scope compress encoding and disorder, which was experimentally shown to be characterized by high compression rate and strong key sensitivity, providing ideas for secrecy and steady communicate in the era of mass information. Literature [21] purpose of assess the influence of graphic recovery on numerical graphic dispose by employing compress techniques and put forward a way that combination the graphic compress and recovery procedure with the aim of improving image quality and reducing storage requirements, illustrating that the proposed method enhance the graphic character and prominent decrease the document size. Literature [22] describes the compressed sensing (CS) technique and its characteristics, which provide higher efficiency than traditional compression reconstruction techniques, and analyzes the restricted isometric property (RIP) and independent iso-distributed property (IID) of the CS technique, emphasizing that the satisfaction of these two properties is a necessary prerequisite for reconstructing the signal. Literature [23] explored graphic compress according to the human eye, the graphic compression method is to delete the superfluous information from the graphic by filtering the graphic with wavelet transform and coding the image using Hoffman method, the simulate consequence emphasize that the size of the graphic can be reduced while achieving the same image effect. Literature [24] introduces vector quantization (VQ) compression as a simple to operate image compression method that can achieve the compression of the graphic to 1/16 of the primitive size and proposes an graphic compress method according to VQ compression, which is effective in improving the compression ratio. Literature [25] describes an image compression and recovery method, which includes a compression phase and a recovery phase, combines Taylor's Factor (Taylor) and Sunflower Optimization (SFO) algorithms to design the Taylor-SFO algorithm and unfolds a performance evaluation of the algorithm pair.

The study improves the genetic algorithm in the multiple-external optimize algorithm, and improves the arithmetic's ability to solve the optimization of image compression and restoration by introducing an accelerated search strategy. The BP neuro mesh is optimizing by improving the genetic arithmetic, and the drill specimen are input to the BP neural mesh and the initial space is encoded. Calculate the adaptation of zooid in the patriarch populace, and then generate the offspring individuals through select, intersect and mutation operations. Combine the enhance heredity arithmetic to perform area seek and iteratively find the optimalizing offspring individuals. By executing the arithmetic, the optimalizing weightings and value range are obtained to train the mesh, and the image compression information is efference from the conceal stratum. Then the efference of the output stratum is calculated from the compressed data to recover the HD image. The feasibility of this paper's method for image compression and recovery is evaluated by PSNR and SSIM on Landscape-16K dataset collected in this paper.

II. Research on multi-objective optimization algorithms

II. A.Multiple-external optimize problem

The mathematic form of the multiple-external optimize problems MOPs [26] is as follows:

$$\begin{aligned} &\min f(x) = (f_1(x), f_2(x), ..., f_m(x))^T \\ &subject\ to\ x \in \Omega \subseteq R^n \end{aligned} \tag{1}$$

In Eq. $\min f(x)$ denotes a set of minimization external equation, and $f_m(x)$ denotes the m th optimization objective function. When $m <= 3$, the question is a multiple-external optimize question MOP, and when $m > 3$, it is called a high-dimensional multi-objective optimization problem MaOP, with $x = (x_1, x_2, ..., x_n)^T$ is an n-dimensional decision vector in the decision space Ω. Based on the MOPs problem model, the following definitions are given:

Implication 1: For two decision vectors $x, y \in \Omega$, if at any $i = 1, 2, ..., m$, there is $f_i(x) \le f_i(y)$, and there existence at least one $j \in 1, 2, ..., m$ that satisfies $f_j(x) < f_j(y)$, then the vector x dominates the vector y.

Definition 2: For a determine complexor $x \in \Omega$, there existence no determine complexor $x' \in \Omega$ dominating the vector x, then the determine complexor x is a Pareto optimalizing resolve.

Definition 3: For a set of decision vectors $PS = \{x_1, x_2, ..., x_k\}$, the decision vectors $x_k \in \Omega$ inside the set are Pareto optimalizing resolve, then PS is said to be a Pareto optimalizing solution set.

Definition 4: The region in the objective space formed by all the decision vectors in the Pareto optimalizing solution set PS of a multiple-external optimize question is called the Pareto front.

Definition 5: Form vector $z^* = (\min f_1, \min f_2, ..., \min f_m)$ by taking all decision vectors $\min f_i$ in the external interspace and call z^* the ideal point.

Definition 6: The decision vectors in the Pareto optimalizing solution set PS in the objective space $\max f_i$ are formed into the vector $z^{nad} = (\max f_1, \max f_2, ..., \max f_m)$, and call z^{nad} the maximum point.

II. B.Multiple-external optimize according to heredity arithmetic

Heredity Arithmetic (GA) [27] is a search and optimize arithmetic that simulation the procedure of biologic devolvement and pertain to the sort of devolvement Arithmetic (EA).

Genetic algorithms utilize the principle of natural selection and the concept of variation in genes to perform a global search with the goal of finding an optimal solution to a problem. The algorithm draws on Darwin's theory of natural evolution, which states that the individual best adapted to a given environment will continue to survive. The genetic algorithm simulates the genetic and evolutionary mechanisms in biological evolution to find the optimalizing resolve to the question through a continuous iterative solution process.

The principle of using genetic algorithms for solving image compression and restoration can be explained as follows: it represents potential solutions to the problem to be solved as unique chromosomes by means of specific coding, i.e., it characterizes each solution by a sequence of genes. The algorithm starts with an initial population that contains several randomly generated chromosomes representing the initial set of solutions to the problem. If a chromosome with sufficiently high fitness is found during the search, the search can be terminated. Otherwise, the algorithm proceeds by eliminating those individuals with low fitness and retaining those with high fitness into the next generation population. Through several genetic operations, namely selection, crossover and mutation, the algorithm continuously performs a global search in the resolve interspace with the objective of finding chromosomes with higher fitness. After a series of evolutionary cycles, the algorithm will elect the DNA with the highest adaptation from the current population and decode it to acquire the optimalizing resolve to the question or an answer that is very close to the optimalizing resolve.

II. C.Multi-objective optimization evaluation index

For evaluate the degree of superiority of a multiple-external optimization arithmetic, it is generally measured in clause of both astringe and pluralism, and the definitions of three performance metrics are given in this section, which will be used in the subsequent experimental simulation section.

(1) Generation Distance (GD): it can measurement the convergence of the non-primary position resolve set, assuming that TF denotes a set of coincident distribution solution sets on the practical Pareto front of the test set, the GD value is defined as follows:

$$GD(PF)=\frac{\sum_{x\in PF}\min_{y\in TF}d(x,y)}{NumPF} \tag{2}$$

where $d(x,y)$ Euclidean length between individuals x and y in the target interspace, and NumPF expression the amount of individuals in the solution set PF.

(2) Inverse Generation length (IGD): it can measurement the astringe and pluralism of the resolve set, and the IGD worth is defined as follows

$$IGD(PF)=\frac{\sum_{x\in TF}\min_{y\in PF}d(x,y)}{NumTF} \tag{3}$$

where NumTF denotes the amount of individuals in the TF solution set, when the amount and distribution of solutions in the solution set PF are very similar to the TF solution set, the value of IGD will be smaller and smaller, so when the value of IGD is smaller, the performance of the algorithm is better.

(3) Frontier contribution ratio (CR): used to quantify the proportion of the Pareto frontier acquired by the arithmetic in the real Pareto frontier. It is defined as follows:

$$CR=\frac{\left|\left\{x\middle|x\in\Omega\cap x\in\Omega^{*}\right\}\right|}{\left|\Omega^{*}\right|}\times 100\% \tag{4}$$

Ω^{*} denotes the true Pareto front, and Ω denotes the Pareto front obtained by the algorithm.

III. Improved multi-objective optimization BP network image compression and recovery techniques

III. A. Genetic Algorithm for Accelerated Search Strategies

Although current genetic algorithms have many advantages, they still have some problems. Such as some optimize question, there is a lack of area search and the optimization results are prone to premature. It is very important to make the algorithm converge quickly and keep the diversity of individuals, and improve the accuracy of prediction.

To address this question, this articl improves on the traditional genetic algorithm and proposes a new method: expedite seek tactics heredity arithmetic (ASSGA).

When the selection operation is carried out, the elite individual migration operator is chosen, which aims to improve the algorithm's global optimization search ability, ensure the advantage of the species and enhance the astringe speed of the arithmetic. The worst zooid after selection are subjected to mutation operation, which enriches the diversity of the populace. The global seek ability of the algorithm is made to be enhanced and the phenomenon of premature maturity of the algorithm is avoided. Segmented point taking for the crossover operator enables the elements of zooid to exchange information evenly. Introduce area seek arithmetic, so that the enhance heredity arithmetic area seek ability becomes stronger.

The enhance idea of the way is mainly to enhance the heredity operator of the traditional heredity arithmetic, so as to solve the problems existing in the traditional genetic algorithm. The enhance arithmetic is able to solve the parameters of the previous neuro mesh pattern globally, and has more advanced computational precision, wider computational range, and faster astringe speed. Figure 1 shows the implementation procedure of the accelerated search strategy genetic algorithm.

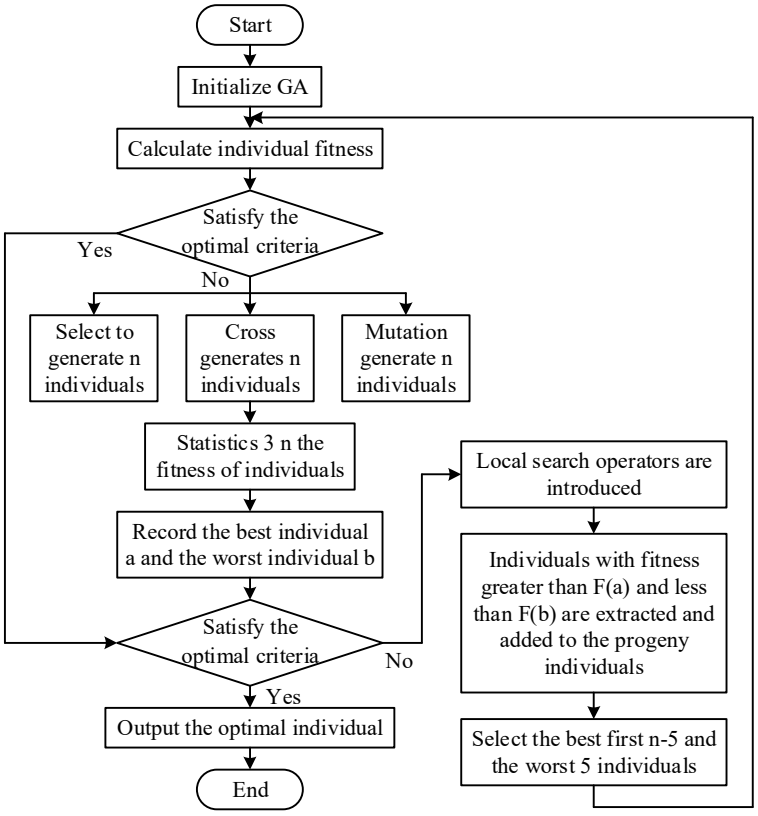

Figure 1: Implementation process of genetic algorithm for accelerated search strategy

III. B. ASSGA optimizing BP neuro mesh

In this section, the traditional heredity arithmetic is improved structurally, and then the enhance heredity arithmetic is applied to optimizing the weightings and value range of the BP neuro mesh [28]. The search way of ASSGA does not need the gradient data required by the traditional BP network, and the algorithm only needs to solve the function solvable under the constraints, and the algorithm can work properly.

The optimization objective formula for ASSGA optimized BP neural network is:

$$\min E(\omega,v,\lambda,\theta,\gamma)=\frac{1}{2}\sum_{i=1}^{N_i}\sum_{k=1}^{n}(d_{ik}-y_{ik})^2 \tag{5}$$

Where d_{ik}, y_{ik} represents the desired and actual efference worth of the mesh, respectively. Where $\omega,v,\lambda,\theta,\gamma$ represents the connection weights from the input stratum to the intermediate stratum, from the first conceal stratum to the second conceal stratum,from the hidden layer to the output layer, the thresholds of each neuron in the hidden layer, and the thresholds of the various transcendental elements in the output layer, respectively. Using these four parameters to find E, if E meets the requirements, then the network model has been trained successfully.

Optimize the traditional BP neural network with ASSGA, the specific implementation steps of the method are as follows: first, set the number of training samples to N, and divide the N training samples into training samples ϕ_1, training samples ϕ_2.

Let the number of test samples ϕ_3 be M:

$$\phi_1 = \{(x_k, y_k) \mid x \in R^m, y \in R^n, k = 1,2,...,N_1, N_1 < N\} \tag{6}$$

$$\phi_2 = \{(x_k, y_k) \mid x \in R^m, y \in R^n, k = N_1 + 1, N_1 + 2,..., N\} \tag{7}$$

Establish the corresponding objective function according to the fitness function, and let the fitness function be $F(\omega, v, \lambda, \theta, \gamma)$ then define the fitness function as:

$$F(\omega, v, \lambda, \theta, \gamma) = \frac{1}{\sqrt{\sum_{i=1}^{N_1}\sum_{k=1}^{n}(d_{ik} - y_{ik})^2}} \tag{8}$$

(1) Normal training of traditional BP neuro mesh to determine the initial solution space, set the number of training times, drill error and test error, and input the training samples into the network. If the training error and test error at this time satisfy the desired conditions at the same time, record the range of weights at this time, and set the maximum and minimum weights as $\mu^{\max}$ and $\mu^{\min}$, respectively. The initial space of weights is determined, and this interval is $[\mu^{\max} - \delta_1, \mu^{\min} + \delta_2]$ (where δ_1 and δ_2 are the adjustment parameters).

(2) The initial solution space is encoded by encoding the initial weights in binary. The weight coefficients serve to control the connection rights of the network. The codes are sequentially concatenated into long strings, each long string corresponding to a set of connection weights.

(3) The initial parent population consists of s individuals which are L uniformly distributed random numbers on the interval $[\mu^{\max} - \delta_1, \mu^{\min} + \delta_2]$. The maximum amount of evolutionary generations for this algorithm is set to T.

(4) Calculate the adaptation of each individual in the parent populace. The smaller the worth of the objective function $f(i)$ of the i th individual is, it means that the larger the worth of the fitness equation $F(\omega, v, \lambda, \theta, \gamma)$ of that individual is, the better the fitness of that individual is. The obtained connection weights are entered into the samples to be trained and the adaptation of each individual is calculated.

(5) The selection, crossover and mutation operations performed on the initial parent individuals respectively, select the i th individual according to the probability $p(i)$, and the number of elect zooid is $n-5$. Then the parent individuals ranked in the top 5 are added to the offspring populace, and the number of new offspring individuals passing the selection operation is n, denoted as $p_1(t)$. A multipoint segmented uniform crossover operation is used to randomly select a pair of parent individuals according to the magnitude of the probability, and multi-point intersect operators are introduced to perform random point intersect of the parent individuals in a fixed partition. Generate n offspring individuals, denoted as $p_2(t)$.

The initial parent individual is subjected to two selective random multipoint mutations, yielding n offspring individuals, denoted $p_3(t)$.

(6) Calculate the fitness value for the $3n$ offspring individuals obtained by selection, crossover, and mutation, and retain the optimal and worst individuals.

(7) Area seek operator, sort the $3n$ offspring individuals obtained from steps (6)-(9) by fitness value in order of size, rank the first n individuals as nodes, set the search range, and find the excellent individuals through local search. If the new individual searched satisfies the criteria, the individual is output and the step ends. If the criterion is not satisfied, the iteration continues.

(8) Iterate and select the $n-5$ individuals at the top of the fitness scale and the 5 individuals with the worst fitness scale to be reintroduced as the new parent population. The algorithm goes to (5) and carries out then iterates steps (4)-(8) repeatedly. Evolution continues to the T th generation.

(9) The individuals in the T th generation group are subjected to the decoding operation, and the L group weight coefficients are obtained by the operation and input into the training samples ϕ_2 to compute the male as:

$$\min E_2(\omega, v, \lambda, \theta, \gamma) = \frac{1}{N_1 - N_2}\sum_{i=1}^{N_2}\sum_{k=1}^{n}(d_{ik} - y_{ik})^2 \tag{9}$$

III. C. Steps for HD photographic image compression and recovery

The ASSGA-BP network is used for image compression and recovery, and the basic model of the ASSGA-BP network is shown in Figure 2. The $n \times n$ in the model indicates the chunk size of the input image, and each pixel point in the image chunk corresponds to an input or output neuron. The basic idea of compression is that the input original image is processed by the implicit layer and output as a compression result, which is saved as image features. For recovery, the image features are output as a reconstructed image through the output layer. Thus the

connection weights from the input layer to the implicit layer are equivalent to an encoder and the connection weights from the implicit layer to the output layer are equivalent to a decoder.

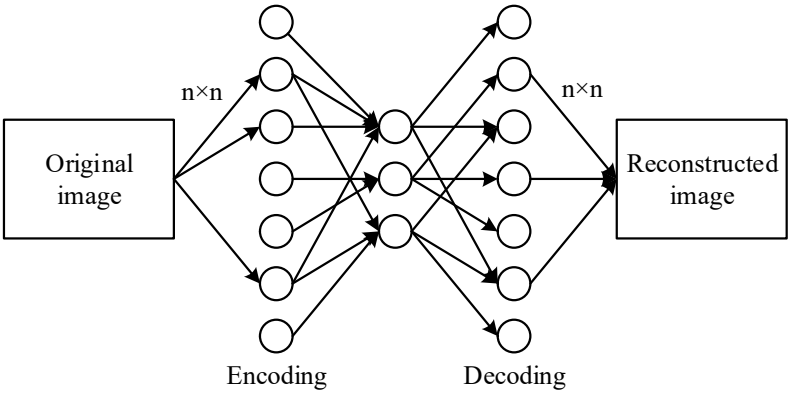

Figure 2: Image compression model based on ASSGA-BP network

Based on the previous study, the steps of ASSGA-BP network image compression and recovery algorithm are:
(1) Chunk the image and normalize it.
(2) Execute the ASSGA-BP network algorithm to obtain the optimal initial weights and thresholds.
(3) Train the network with the optimal initial weights and thresholds.
(4) Calculate the output of the hidden layer and save the compressed data.
(5) Load the compressed data and compute the output of the output layer.
(6) Inverse normalize the output data and recover the image from the data block.

IV. Analysis of the effect of high-definition image compression and recovery in ASSGA-BP network

IV. A. Image compression and recovery evaluation index

Peak Signal to Noise Ratio (PSNR) as well as Structural Similarity Index (SSIM) are used to evaluate the image compression and restoration capability of the network model above.

PSNR is a measure of image quality. In this section, the fitness value of the ASSGA-BP network model is defined as the average of the PSNR values of all the compressed and recovered images obtained by this network at the end of its training on the training set. The Peak Signal to Noise Ratio is calculated as in Eq:

$$PSNR = 10 \times \log_{10}\left(\frac{(2^n - 1)^2}{MSE}\right) \tag{10}$$

where, MSE is the mean square error between the original image and the denoised image, and n denotes the number of image sampling points. PSNR takes the value in the range of 20-40dB, and the larger the value of PSNR, the better the quality of the image.

SSIM measures image similarity in terms of brightness, contrast and structure respectively. The mean value is used as an estimate of brightness, standard deviation as an estimate of contrast, and covariance as a measure of structural similarity. SSIM takes the value in the range of [0, 1], and the larger the value, the smaller the image distortion and the more similar the image is. SSIM is computed as Eq:

$$SSIM(x, y) = \frac{(2\mu_x\mu_y + C_1)(2\sigma_{xy} + C_2)}{(\mu_x^2 + \mu_y^2 + C_1)(\sigma_x^2 + \sigma_y^2 + C_2)} \tag{11}$$

where C_1 and C_2 are constants. μ_x and μ_y are the mean of the images x and y, σ_x and σ_y are the variances of the images x and y, and σ_{xy} is the covariance of the images x and y.

IV. B. Test data set and parameter settings

The proposed BP network based on improved multi-objective optimization algorithm is trained, tested and validated using the publicly available HD photographic image dataset Landscape-16K.The Landscape-16K dataset consists of 16,000 high-definition bleak landscape images with a resolution $\geqslant$ 4K. Among them, 70% are set as training set, 15% as testing set, and 15% as validation set. Since there is a certain amount of noise in the actual HD images, Gaussian noise with standard deviation $\sigma = 20$ is used to simulate the noise in the images.

In order to verify the performance of the proposed BP network based on improved multi-objective optimization algorithm, it is compared with the multi-objective based differential evolutionary algorithm (DE), genetic algorithm (GA), hybrid teach-and-learn algorithm (TLBO), and particle swarm algorithm (PSO) for comparative image compression and recovery comparison. The population size N is set to 30 and the number of evolutionary generations T is set to 15.

The experimental running environment of this study is Ubuntu 20.04.3LTS operating system, CPU is Intel(R)Xeon(R)Silver4214CPU@2.20GHz, memory is 32GRAM, and graphics card is NVIDIACorporationGeForceRTX2080Ti.The multi-objective hybrid evolutionary algorithm was developed using the TensorFlow framework running on Visual Studio Code software for 10 hours.

IV. C. Experimental results and analysis

IV. C. 1) Analysis of the effectiveness of image compression and recovery search strategies

In order to verify the effectiveness of the improved multi-objective optimization algorithms in this paper, the traditional multi-objective optimization algorithms above are selected in the comparison experiments, which are Differential Evolutionary Algorithm (DE), Genetic Algorithm (GA), Hybrid Teaching and Learning Algorithm (TLBO), Particle Swarm Algorithm (PSO), and the analysis of the effectiveness is carried out.

In the simulation experiment, all algorithms were run independently for 30 times, and the average value of the evaluation index was calculated. The running time of all algorithms was set to 300 seconds. The statistical results of generation distance (GD), inverse generation distance (IGD) and frontier contribution rate (CR) are shown in Fig. 3, Fig. 4 and Fig. 5, respectively.

From the data in Figures 3 and 4, it can be seen that the generation distance and inverse generation distance of this paper's algorithm, ASSGA-BP, are 0.0312 and 0.0703, respectively, which are smaller than the comparison model. From Fig. 5, it can be seen that the frontier contribution rate of ASSGA-BP is 61.96%, which is 17.90%~37.66% higher than the comparison algorithm, and much larger than the traditional multi-objective optimization algorithm. Therefore, compared with the traditional multi-objective optimization algorithm, the Pareto frontier solution obtained by ASSGA-BP has better convergence and comprehensive performance with higher frontier contribution rate.

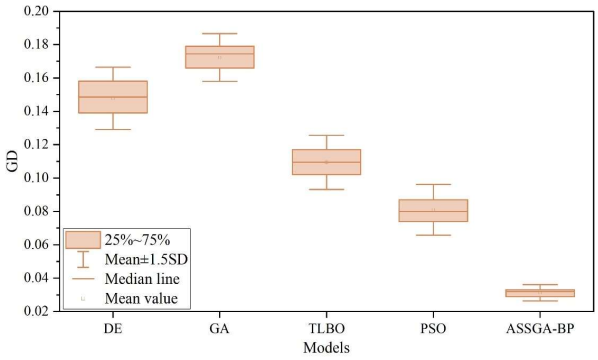

Figure 3: Different models GD value statistics

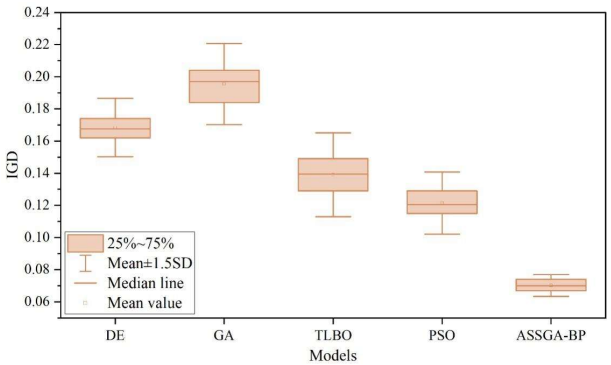

Figure 4: Different models IGD value statistics

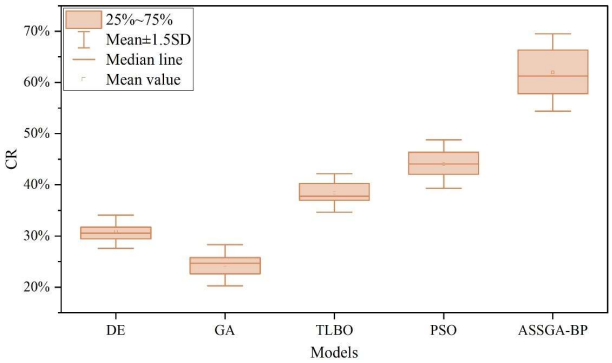

Figure 5: Different models CR value statistics

Table 1 shows the results of the validity experiment solution set coverage. From the table, it can be obtained that the solution set coverage rates c(ASSGA-BP, DE), c(ASSGA-BP, GA), c(ASSGA-BP, TLBO), and c(ASSGA-BP, PSO) are 0.56, 0.62, 0.79, and 0.68, respectively, which are much larger than the coverage rates c(DE, ASSGA-BP), c(GA, ASSGA- BP), c(TLBO, ASSGA-BP), and c(PSO, ASSGA-BP) measured values. It is shown that the Pareto frontier solutions of ASSGA-BP cover the Pareto frontier solutions of DE, GA, TLBO, and PSO in a large number of cases. Taken together, ASSGA-BP outperforms the traditional multi-objective optimization algorithm in all indicators.

Based on the above analysis, it can be concluded that the proposed accelerated search strategy BP network plays a role in improving all performance indexes.

Table 1: Validity test solution set coverage result

Indicators	Results	Indicators	Results
c(ASSGA-BP,DE)	0.56	c(DE,ASSGA-BP)	0
c(ASSGA-BP,GA)	0.62	c(GA,ASSGA-BP)	0.13
c(ASSGA-BP,TLBO)	0.79	c(TLBO,ASSGA-BP)	0.09
c(ASSGA-BP,PSO)	0.68	c(PSO,ASSGA-BP)	0

IV. C. 2) Comparative analysis of compression performance

This section plots the rate-distortion performance curves of the ASSGA-BP method proposed in this paper and the traditional multi-objective optimization comparison method for PSNR metrics and MS-SSIM metrics on Landscape-16K dataset, respectively.MS-SSIM is improved from SSIM, and has been verified to measure distortion more accurately.MS-SSIM introduces a multi-scale computation to simulate the effect of different scales by different MS-SSIM introduces a multi-scale calculation to expand the receptive field by different sizes of filter operators to simulate the effect of different scales, and realizes the stable performance when the image resolution is different. The calculation formula is as follows:

$$MS-SSIM(x,x')=\left[l_M(x,x')\right]^{\alpha M}\prod_{j=1}^{M}\left[c_j(x,x')\right]^{\beta j}\left[s_j(x,x')\right]^{\gamma j} \tag{12}$$

where $l(x,x')$ represents brightness comparison, $c(x,x')$ represents contrast comparison, and $s(x,x')$ represents structural similarity comparison.The value range of MS-SSIM also ranges from 0 to 1, but due to the small range of variation of its value, which mainly focuses on the range of 0.8 to 1 in the experiments of this paper, the metric effect is not obvious, and in order to emphasize the gap, it is converted to the value of unit decibel. It is converted to a value with unit of decibel, and the conversion formula is:

$$MS-SSIM(db)=-10\log_{10}(1-MS-SSIM) \tag{13}$$

Fig. 6 plots the rate distortion performance curves of different methods on Landscape-16K dataset, which shows the comparison results of these two metrics for different methods at different bit rates. From the figure, it can be seen that under the same degree of image compression (bpp), the methods in this paper have obvious performance improvement in PSNR and MS-SSIM metrics compared to DE, GA, TLBO and PSO methods.

Specifically, when bpp is 1, in PSNR metric, this paper's method has an improvement of 3.31-9.13 db compared with traditional multi-objective optimization algorithms. In terms of MS-SSIM metrics, the improvement of this paper's method is gradually obvious with the increase of bpp. When bpp is 1, MS-SSIM reaches 23.24db, which is

significantly better than the comparison method. Meanwhile, this paper's method has performance improvement on the interval of bpp from 0 to 1, which can verify the effectiveness of the method in this section.

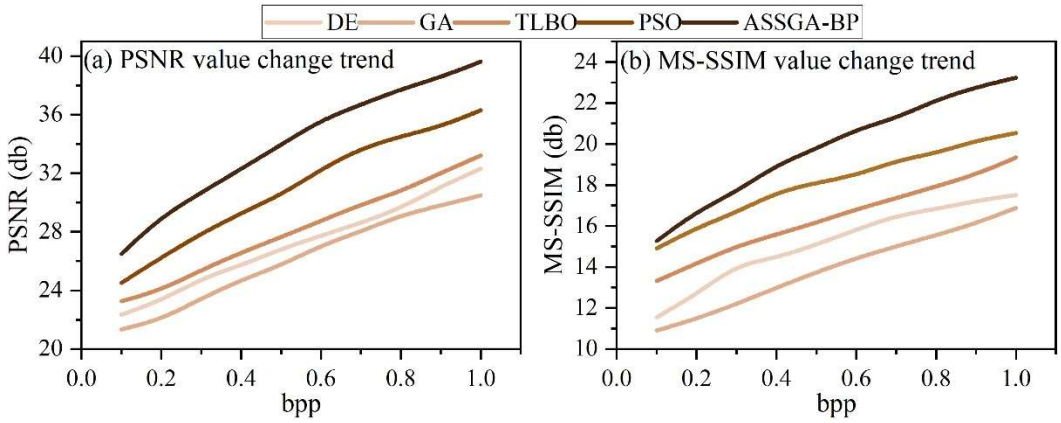

Figure 6: Different methods of distortion performance curves in data sets

In this section, five images from Landscape-16K dataset are randomly selected to quantitatively analyze the compression performance of different methods. The traditional multi-objective optimization algorithm above is also selected to compare with the ASSGA-BP method proposed in this paper. Five images were tested under similar bpp, and the experimental results of the compression performance of some images in the dataset are shown in Fig. 7.

As can be seen from the figure, the ASSGA-BP method has the highest PSNR and MS-SSIM metrics for reconstructed images at similar bpp. For example, for image 1, the PSNR metric of the ASSGA-BP method is 30.45db and the MS-SSIM metric is 0.91. Comparing with the traditional multi-objective optimization method, the PSNR improves by 2.04-10.33db and the MS-SSIM improves by 0.02-0.09. Further analysis of the experimental results shows that this paper optimizes the model for the MSE when training the model, while the PSNR is essentially a more intuitive representation of the MSE between the original image and the reconstructed image, so the evaluation index will be more in favor of PSNR, so the final model trained in this paper compared with the comparison method, the PSNR index is improved significantly, but the MS-SSIM index is only slightly improved.

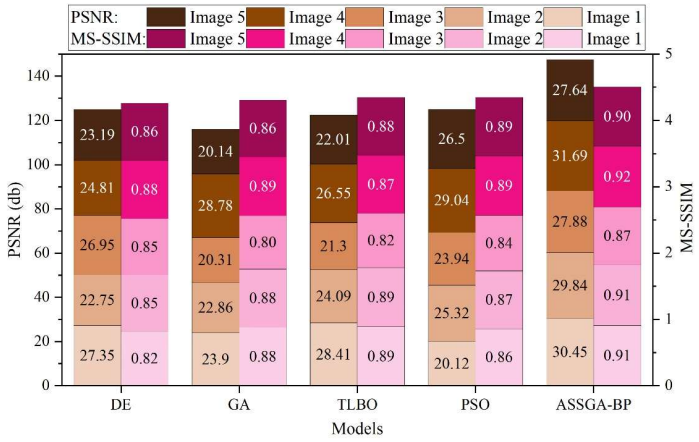

Figure 7: The results of the compression of the data collection

IV. C. 3) Qualitative Visual Analysis of Image Recovery

In order to visualize the effectiveness of this paper's model ASSGA-BP on image recovery tasks, this paper applies it in in a variety of tasks and demonstrates the actual effect of image recovery of ASSGA-BP model through visualization. The traditional multi-objective optimization algorithm mentioned above is chosen to compare with this paper's model for recovery visualization. The image recovery tasks include:

(1) Image dehaze: haze usually leads to image blurring, contrast reduction and color distortion. Image defogging aims to eliminate the visual impact of atmospheric haze and restore the clarity and color of images taken under hazy conditions.

(2) Image De-Rain: Rain usually results in scenes with rain speckled occlusions, streaks and blurred areas. The Image De-Rain task is designed to remove interference in the image due to rainfall and improve the visibility of the image.

(3) Image De-Snowing: Snowflakes usually appear as white particles or specks in the image, affecting the overall visual effect of the scene. The goal of the image de-snowing task is to eliminate visual interference in the image due to snowfall.

(4) Image Deblurring: Due to motion or inaccurate focusing, etc., the captured image shows phenomena such as motion blur and out-of-focus blur. Image deblurring aims to restore clear details in reconstructed images.

(5) Low-light Image Enhancement: Shot under insufficient lighting conditions, the resulting image often exhibits problems such as high noise, low contrast, and lack of detail. The low-light image enhancement task aims to restore the visibility and details of such images.

The following is a quantitative comparison of the overall performance of ASSGA-BP with the evaluation metrics of other methods on five types of image restoration tasks. Comparisons against PSNR and SSIM are used to demonstrate the overall effectiveness of ASSGA-BP on the image restoration task.

Figures 8 and 9 show the results of the comparison of PSNR and SSIM metrics for the overall effectiveness on five types of image recovery tasks, respectively. Combining the two figures, it can be seen that the method in this paper achieves relatively excellent results in each image recovery task. In particular, it performs well in the image snow removal and enhancement tasks, with a PSNR of 34.76db, 33.28db, and a SSIM of 0.847, 0.846 in the two types of restoration tasks, respectively.This paper's model performs well in multi-task processing, indicating that it has strong versatility and stability, and the experimental results also validate its effectiveness in dealing with the complexity of multiple restoration tasks.

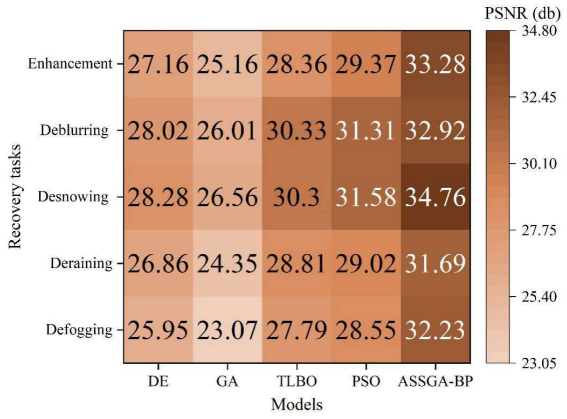

Figure 8: The overall effect of the PSNR index was improved

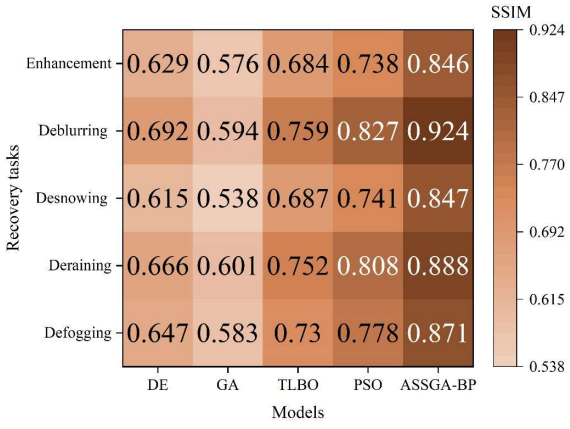

Figure 9: The overall effect of the SSIM index was improved

V. Conclusion

In this paper, for the shortcomings of genetic algorithm in HD image compression and recovery, we propose an improved genetic algorithm (ASSGA) to accelerate the search, and fuse it with BP neural network to construct an all-media fusion image compression and recovery strategy based on ASSGA-BP network. The improved genetic algorithm is utilized to globally solve the parameters of the neural network model to enhance the convergence speed of the algorithm. The objective function of image compression and recovery is established according to the fitness function, and the better sample individuals are screened by selection, crossover, mutation and other operational steps. Through the hidden layer in the neural network, the original image is processed and the compression result is output, and then the image features are recovered to high-definition images through the output layer to realize the complete image compression and recovery process. The average frontier contribution rate of the ASSGA-BP model is 61.96%, which is more than 15% higher than that of the comparison algorithm. And the c(ASSGA-BP, DE) solution set coverage is much larger than c(DE, ASSGA-BP). When the compression degree is 1, the PSNR and MS-SSIM of this paper's method are improved by 3.31-9.13db and 2.71-6.35db, respectively, compared with the comparison method. And it achieved the best results in the overall effect PSNR, SSIM metrics for different image recovery tasks, with the best performance in the image de-snowing and enhancement tasks.

References

[1] Shonhe, L. (2017). A literature review of information dissemination techniques in the 21st century era. Library Philosophy and Practice (e-journal), 1731.

[2] Oyighan, D., & Okwu, E. (2024). Social media for information dissemination in the digital era. RAY: International Journal of Multidisciplinary Studies, 10(1), 1-21.

[3] Hanhart, P., Bernardo, M. V., Pereira, M., G. Pinheiro, A. M., & Ebrahimi, T. (2015). Benchmarking of objective quality metrics for HDR image quality assessment. EURASIP Journal on Image and Video Processing, 2015, 1-18.

[4] Metzler, C., Mousavi, A., & Baraniuk, R. (2017). Learned D-AMP: Principled neural network based compressive image recovery. Advances in neural information processing systems, 30.

[5] Surabhi, N., & Unnithan, S. N. (2017). Image compression techniques: a review. International Journal of Engineering Development and Research, 5(1), 585-589.

[6] Al-jawaherry, M. A., & Hamid, S. Y. (2021). Image Compression techniques: literature review. Journal of Al-Qadisiyah for computer science and mathematics, 13(4), Page-10.

[7] Rippel, O., & Bourdev, L. (2017, July). Real-time adaptive image compression. In International Conference on Machine Learning (pp. 2922-2930). PMLR.

[8] Rahman, M. A., & Hamada, M. (2019). Lossless image compression techniques: A state-of-the-art survey. Symmetry, 11(10), 1274.

[9] Bai, Y., Liu, X., Wang, K., Ji, X., Wu, X., & Gao, W. (2024). Deep lossy plus residual coding for lossless and near-lossless image compression. IEEE Transactions on Pattern Analysis and Machine Intelligence, 46(5), 3577-3594.

[10] Jamil, S., Piran, M. J., Rahman, M., & Kwon, O. J. (2023). Learning-driven lossy image compression: A comprehensive survey. Engineering Applications of Artificial Intelligence, 123, 106361.

[11] Krivenko, S. S., Krylova, O., Bataeva, E., & Lukin, V. V. (2018). Smart lossy compression of images based on distortion prediction. Telecommunications and Radio Engineering, 77(17).

[12] Joshi, M., Agarwal, A. K., & Gupta, B. (2019). Fractal image compression and its techniques: a review. Soft Computing: Theories and Applications: Proceedings of SoCTA 2017, 235-243.

[13] Parmar, C. K., & Pancholi, K. (2015). A review on image compression techniques. Journal of Information. Knowledge and Research in Electrical Engineering, 2(2), 281-284.

[14] Wiseman, Y. (2015). Improved JPEG based GPS picture compression. Advanced Science and Technology Letters, 85, 59-63.

[15] Singh, A. P., Potnis, A., & Kumar, A. (2016). A review on latest techniques of image compression. International Research Journal of Engineering and Technology (IRJET), 3(7), 2395-0056.

[16] Zamir, S. W., Arora, A., Khan, S., Hayat, M., Khan, F. S., Yang, M. H., & Shao, L. (2022). Learning enriched features for fast image restoration and enhancement. IEEE transactions on pattern analysis and machine intelligence, 45(2), 1934-1948.

[17] Potlapalli, V., Zamir, S. W., Khan, S. H., & Shahbaz Khan, F. (2023). Promptir: Prompting for all-in-one image restoration. Advances in Neural Information Processing Systems, 36, 71275-71293.

[18] Tohidi, F., Paul, M., & Hooshmandasl, M. R. (2021). Detection and recovery of higher tampered images using novel feature and compression strategy. IEEE Access, 9, 57510-57528.

[19] Li, Q., Fu, Y., Zhang, Z., Fofanah, A. J., & Gao, T. (2022). Medical images lossless recovery based on POB number system and image compression. Multimedia Tools and Applications, 81(8), 11415-11440.

[20] Wen, H., Ma, L., Liu, L., Huang, Y., Chen, Z., Li, R., ... & Zhang, C. (2022). High-quality restoration image encryption using DCT frequency-domain compression coding and chaos. Scientific Reports, 12(1), 16523.

[21] Sohal, J., Sahoo, G. S., Jain, S. K., Kalpana, B., & Wawage, P. S. (2023, December). Evaluating the Impact of Image Restoration on Digital Image Processing Using compression Technique. In 2023 3rd International Conference on Smart Generation Computing, Communication and Networking (SMART GENCON) (pp. 1-6). IEEE.

[22] Upadhyaya, V., & Salim, M. (2020). Compressive Sensing: An Efficient Approach for Image Compression and Recovery. In Recent Trends in Communication and Intelligent Systems: Proceedings of ICRTCIS 2019 (pp. 25-34). Singapore: Springer Singapore.

[23] Yuan, S., & Hu, J. (2019). Research on image compression technology based on Huffman coding. Journal of Visual Communication and Image Representation, 59, 33-38.

[24] Xu, S., Chang, C. C., & Liu, Y. (2021). A novel image compression technology based on vector quantisation and linear regression prediction. Connection Science, 33(2), 219-236.
[25] Optimization-Based, T. S. F. (2023). Compressive Sensing for Image Compression and Recovery. The Computer Journal, 66(4).
[26] Zhenxing Yu,Qinwei Fan,Jacek M. Zurada,Jigen Peng,Haiyang Li & Jian Wang. (2025). Solving sparse multi-objective optimization problems via dynamic adaptive grouping and reward-penalty sparse strategies. Swarm and Evolutionary Computation,94,101881-101881.
[27] Michelle Setiyanti,Genrawan Hoendarto & Jimmy Tjen. (2025). Enhancing Water Potability Identification through Random Forest Regression and Genetic Algorithm Optimization. Engineering Headway,18,101-110.
[28] Qiong Li,Rui Su,Hongxia Qiao,Li Su,Penghui Wang & Linhan Gong. (2025). Prediction of compressive strength and porosity of vegetated concrete based on hybrid BP neural networks. Materials Today Communications,44,112080-112080.